9-22-2014

Laboratory measurements of contact freezing by dust and bacteria at temperatures of mixed-phase clouds

Joseph Niehaus
Michigan Technological University

John Becker
Michigan Technological University

Alexander Kostinski
Michigan Technological University

Will Cantrell
Michigan Technological University

Recommended Citation

Niehaus, J., Becker, J., Kostinski, A., & Cantrell, W. (2014). Laboratory measurements of contact freezing by dust and bacteria at temperatures of mixed-phase clouds. *Journal of the Atmospheric Sciences, 76*(3), 3659-3667. http://dx.doi.org/10.1175/JAS-D-14-0022.1
Retrieved from: https://digitalcommons.mtu.edu/physics-fp/179

Follow this and additional works at: https://digitalcommons.mtu.edu/physics-fp

 Part of the Physics Commons

Laboratory Measurements of Contact Freezing by Dust and Bacteria at Temperatures of Mixed-Phase Clouds

JOSEPH NIEHAUS

Atmospheric Sciences Program, Michigan Technological University, Houghton, Michigan

JENNIFER G. BECKER

Civil and Environmental Engineering, Michigan Technological University, Houghton, Michigan

ALEXANDER KOSTINSKI AND WILL CANTRELL

Atmospheric Sciences Program, and Physics, Michigan Technological University, Houghton, Michigan

(Manuscript received 6 February 2014, in final form 3 July 2014)

ABSTRACT

Laboratory measurements of freezing by aerosol particles in contact mode are presented. The fraction of particles catalyzing freezing is quantified for three mineral dusts and three strains of bacteria. This is the most comprehensive such dataset to date for temperatures greater than −20°C, relevant for warm, mixed-phase clouds. For Arizona Test Dust, feldspar, or rhyolitic ash, more than 10^3 particles are required to initiate a freezing event at −20°C in the contact mode. At −15°C, more than 10^5 particles are required. An ice-negative strain of *Pseudomonas fluorescens* is an order of magnitude more effective than the mineral dusts at every temperature tested. To the best of the authors' knowledge, this is the first measurement of contact-mode freezing by an ice-negative bacterium. An ice-positive strain of *Pseudomonas syringae* reaches its maximum nucleating efficiency, $E = 0.1$, 12°C higher than does *Pseudomonas fluorescens*. This is consistent with the behavior of ice-negative and ice-positive bacteria in the immersion mode, as discovered 40 years ago. Surprisingly, cells of the ice-positive strain *Pseudomonas syringae* CC94 that do not express the ice nucleation active gene showed no contact-freezing activity, whereas the cells of the ice-negative strain of *Pseudomonas fluorescens* showed significant activity.

1. Introduction

Ice formation in the troposphere usually proceeds through heterogeneous pathways, where the presence of a foreign substance catalyzes freezing for supercooled cloud droplets. However, in mixed-phase clouds ice has been observed to form and persist under conditions indicative of heterogeneous nucleation that have yet to be replicated in laboratories (Hoose and Möhler 2012; Ladino Moreno et al. 2013). The details of how ice is initiated and sustained in those warmer clouds are still elusive. Lohmann (2002) and Korolev et al. (2003), for example, find that the deposition and immersion modes of ice nucleation are inactive for the temperatures of midtropospheric clouds. The number of particles that trigger freezing [commonly called ice nuclei (IN)] in the immersion mode was too low to account for all the ice particles observed. The contact mode has been found to catalyze freezing for higher temperatures than immersion mode and may contribute to warm tropospheric ice formation, but quantitative data by which that hypothesis could be tested are lacking (Yun and Penner 2012).

In contact nucleation, a solid particle catalyzes freezing of a supercooled liquid by being in contact with the liquid's surface, whereas the immersion mode is characterized by the particle's complete submersion within the liquid. Direct comparison of the contact and immersion mode has shown that the contact mode is more effective for temperatures down to −34°C (Hoffmann et al. 2013a; Fukuta 1975; Pitter and Pruppacher 1973; Ladino et al. 2011; Fornea et al. 2009). However, the role of contact nucleation remains to be parameterized in a physically

Corresponding author address: Will Cantrell, Michigan Technological University, 1400 Townsend Dr., Houghton, MI 49931.
E-mail: cantrell@mtu.edu

DOI: 10.1175/JAS-D-14-0022.1

motivated way due to a lack of reproducible results in the laboratory and an incomplete theoretical basis for the mechanism.

The earliest experiments with contact freezing showed that it was effective at higher temperatures than was the immersion mode, but the number of particle–droplet interactions was not well documented in those studies (Gokhale and Goold 1968). Subsequent studies provided constraints on the number and size of particles required to initiate freezing (Pitter and Pruppacher 1973; Fukuta 1975), though uncertainties were still substantial. More recently, investigators have approached the problem with the explicit goal of quantifying the number of particle-to-droplet collisions leading to freezing, with varying degrees of success (Svensson et al. 2009; Ladino et al. 2011; Bunker et al. 2012; Hoffmann et al. 2013b). The efficiencies (explained in section 2b) reported by different experiments still show a wide variability, which has prevented an accurate assessment of contact nucleation in the atmosphere.

Little is known about contact-mode nucleation by mineral dust and other inorganic substances, and even less is known about the effectiveness of biological ice nuclei in contact mode (Levin and Yankofsky 1983). A wide range of organisms and biological materials can act as ice nuclei (Després et al. 2012); however, bacteria may be among the most important biological ice nuclei in the atmosphere because they have relatively long atmospheric residence times (due to their small size relative to other biological material like pollen grains), and they can nucleate ice at temperatures up to −2.5°C. Only a few fungal species are known to nucleate ice at comparable temperatures. A growing number of bacteria isolated from air, precipitation, and other habitats have been shown to exhibit ice nucleation properties. However, the most effective ice-nucleating bacteria isolated so far are affiliated with four genera within the Gammaproteobacteria: *Pseudomonas*, *Erwinia*, *Xanthomonas*, and *Pantoea* (Joly et al. 2013). These organisms generally grow in association with plants, and many strains are plant pathogens.

The ice-nucleating activity of these bacteria is catalyzed by a protein located on the cell's outer membrane. Although ice formation may be catalyzed by a single ice-nucleating protein at −12°C, a large aggregate of proteins, which is stabilized by the outer membrane, is required to nucleate ice at a temperature of −3°C (Lagriffoul et al. 2010). Thus, whole bacterial cells may be needed to cause freezing at the highest temperatures. Several factors may affect the size of the ice-nucleating protein complex (e.g., the composition of the culture medium and the conditions under which the bacteria were grown and/or stored). Furthermore, not every cell of a given strain will contain the protein responsible for ice nucleation at a given time. The fraction of cells that nucleate ice ranges from approximately 10^{-8} to close to 1 in different strains (Després et al. 2012). Therefore, ice-nucleating bacteria exhibit a wide range of efficiencies at different temperatures.

We report, based on laboratory experiments, the amount of aerosol that impacts the surface of a supercooled water droplet before catalyzing freezing, in terms of both number of particles and total surface area collected. We find that mineral dusts [Arizona Test Dust (ATD), feldspar, and rhyolitic ash] in the size range from 0.3 to 10 μm are particularly poor contact nuclei for temperatures ranging from −15° to −22°C. The ice-negative bacterium *Pseudomonas fluorescens* strain A506 is a more effective ice nucleus than any of the mineral dusts. Snomax (Snomax International), *Pseudomonas syringae*, is the most active and can form ice up to temperatures of −3.0°C. Another ice-positive *P. syringae* strain (CC94) showed no contact-mode freezing behavior.

2. Methods

a. Measurement

To measure ice nucleation, we employ a cold stage to supercool water droplets before exposing them to aerosol for particle–droplet interactions. We briefly explain the technique here, but it is described in more detail in Niehaus et al. (2013). A 5-μL water droplet [high-performance liquid chromatography (HPLC) grade is placed on a salinized glass slide that sits atop a temperature-controlled copper stage, the contact ice nucleation chamber (CINC). The droplet is supercooled to a specified temperature and allowed to equilibrate with its surroundings. Aerosol is then generated by dispersing dry dust via a vibrating membrane. Filtered air flows through the volume above the vibrating membrane, picking up particles. The aerosol flow is cooled with a heat exchanger, and then directed across the droplet. Some of the particles in the airstream deposit to the droplet, thereby allowing us to evaluate contact freezing. The phase of the droplet is monitored via a 1-mW diode laser focused through the droplet and into a photodiode. When the droplets freeze, the laser beam is scattered and a corresponding drop in signal is observed.

The number of particles that deposit to the droplet is obtained by examining the residue of some test droplets with a scanning electron or optical microscope, similar to the empirical measures employed by Hoffmann et al. (2013b). A total of 5 ± 3 out of every 1000 particles are deposited to the droplet (Niehaus et al. 2013). Knowing the fraction of aerosol particles that deposit to the

droplet, we can determine the number of particles that have collided with a test drop simply by measuring the number of particles passing through the system. That is done with a TSI Optical Particle Sizer (OPS) 3330, which reports particle counts with an uncertainty of 10%.

Once particles are on the surface of the droplet, they can be swept into the interior by air currents or diffusion, conceivably then leading to immersion freezing. To eliminate contributions to nucleation from the immersion mode, we ran experiments in which we sampled aerosol for some time, ensuring that particles were deposited to the droplet. We then switched to a particle-free flow, observing the unfrozen droplet. We detected no freezing events in any of those cases, despite the fact that there were particles immersed in the droplet. As a further control, in some tests, droplets that had frozen by contact nucleation were melted, then cooled back to the original temperature, where freezing was originally observed. The supercooled droplets were then held at a constant temperature for an hour with no aerosol flow; in those cases, the test droplets did not freeze. These tests indicate that the freezing events we observe are the result of a particle–droplet collision, not merely the presence of aerosol particles within the droplet or at its surface.

Because the droplet sits on a glass slide, the surface provides a bound on the achievable supercooling. The heterogeneous freezing temperature due to the glass slide is 249.75 K (−23.5°C), and control tests with droplets can be set to 250.25 K (−23°C) with no observed freezing events. Tests are performed at constant temperature with aerosol flowing past the droplet for 30 min or until a freezing event is observed. Droplets do not evaporate appreciably during this time period, which minimizes changes in the geometry of the system that might affect collision rates of aerosol particles. The number of aerosol particles that collide with the droplet sets an upper limit to the temperature that we can reasonably explore. If the freezing probability for a single particle–droplet collision is low ($E < 10^{-5}$; see section 2b for definitions), the time required to acquire statistically meaningful data is prohibitive.

Our system is designed as a way to measure the probability that an aerosol particle coming into contact with a surface of supercooled water will result in a freezing event. The test droplets that we employ are much, much larger than typical cloud droplets, which are approximately 10 μm in diameter. However, insofar as surface curvature does not play a role in the mechanism of contact nucleation, our measurements are applicable to the case of aerosol particles interacting with cloud droplets. Similarly, aerosol particles in clouds are collected by droplets by thermodiffusiophoresis and gravitational settling of the cloud droplets in a turbulent flow, whereas in the CINC, the particles diffuse and settle out of the airstream onto the test droplets. Finally, clouds are also close to saturation, whereas the airflow in the CINC is dry. Aerosol particles that come into contact with the test droplet must, however, pass through a saturated vapor field surrounding the droplet. Cooper (1974) estimated that the water adsorbed to an aerosol particle would come into equilibrium with a vapor field within 10^{-4} seconds, so we are confident that the particles that hit the test droplets are representative of particles with adsorbed water in a cloud. For a more comprehensive discussion of the distinction between laboratory experiments and contact freezing in clouds, see Ladino Moreno et al. (2013).

b. Freezing efficiency

Contact ice nucleation is quantified by the number efficiency E, defined as the ratio of freezing events F to the number of particles N on or in the droplet,

$$E = \frac{F}{N}. \tag{1}$$

We interpret an efficiency of 10^{-3} to mean that 1 in every 1000 particle impacts results in the droplet freezing.

Heterogeneous nucleation is generally related to surface area, expressed in units of freezing events per time per area (Lamb and Verlinde 2011). Therefore, we have also quantified the efficiency in terms of surface area via

$$\mathrm{SE} = \frac{F}{S_A}, \tag{2}$$

where SE is the number of freezing events per total surface area deposited to the test droplet S_A. In essence, SE is the active site density in contact mode. Note that we are implicitly adopting a singular model in that we assume that a particle that catalyzes freezing in contact mode does so immediately upon interaction with the surface of the droplet; that is, there is no time dependence.

c. Samples

Arizona Test Dust (Powder Technologies Inc.) was chosen because it is well studied and compositionally similar to the dust in many deserts. K-Feldspar's importance was recently quantified by Atkinson et al. (2013), who proposed that the fraction of feldspar in dust dominates a sample's immersion nucleation rate. Rhyolitic ash is volcanic in origin and is known to be glassy; energy dispersive X-ray spectroscopy showed our sample to contain a majority of SiO_2. Aluminum and sulfur were also present.

Several *Pseudomonas syringae* strains have been well characterized in terms of their ice-nucleating ability (Levin and Yankofsky 1983; Maki et al. 1974); therefore, two of them were included in the present study. Snomax is a commercially available product that is added to water to facilitate snowmaking. Strain 31a (ATCC 53543) is presumed to be used in the production of Snomax (Lagriffoul et al. 2010). Freeze-dried cells that are killed via irradiation compose the finished product. The cells are mostly intact, but Snomax also includes cell debris and dried culture medium (Morris 2012). *P. syringae* CC94 was obtained from D. Sands (Montana State University) and maintained as described below. BlightBan (Nufarm Americas) is a biological control agent intended to reduce damage to fruit trees caused by fire blight and frost; it consists of *Pseudomonas fluorescens* strain A506 that naturally lacks the gene responsible for high-temperature ice nucleation.

P. syringae CC94 was routinely maintained at 20°C on agar plates prepared with King's medium B (KB; King et al. 1954). Freeze-dried *P. syringae* CC94 cells were prepared from suspended cultures grown overnight in KB broth in a shaking incubator maintained at 20°C and 160 revolutions per minute (rpm). The cultures were centrifuged at 6000 rpm for 15 min, and the resulting pellet was resuspended in sterile water (1 mL) and transferred to 12-mL conical glass tubes. The aqueous cell suspension was shell frozen in a dry ice and acetone bath and then lyophilized. The freeze-dried pellets were gently crushed with a mortar and pestle to facilitate aerosolization in the vibrating-membrane dust generator.

As noted above, all samples are dry dispersed using a vibrating plastic membrane into a filtered airstream with a dewpoint temperature less than −40°C. The samples that we observed with the OPS were a convolution of the original dust, the efficiency with which that dust is lofted in the airstream by the vibrating membrane, and the efficiency with which the airborne particles are carried through the sampling lines and the contact IN chamber. Particles in the size range $0.5 < D_p < 8.0\,\mu$m dominate the number distributions, which we measure.

3. Results and discussion

The two plots shown in Fig. 1 are number (top) and surface area (bottom) efficiencies for the dust and bacteria. One conclusion evident from both plots is that a significant amount of dust needs to impact the surface before a freezing event occurs. At −20°C, only 1 in about 10^4 mineral dust particles will catalyze freezing, which seems to contradict earlier work that showed mineral dusts were effective in contact mode at temperatures as high as −4°C (Gokhale and Goold 1968; Gokhale and Spengler 1972; Fukuta 1975; Pitter and Pruppacher 1973). The earlier results, however, rarely quantified how many particles were necessary to initiate the phase transition. In some cases, the dusts were manually sprinkled over droplets on a cold plate; as a result, there were undoubtedly many more particles on the surface of their test droplets than are represented in Fig. 1.

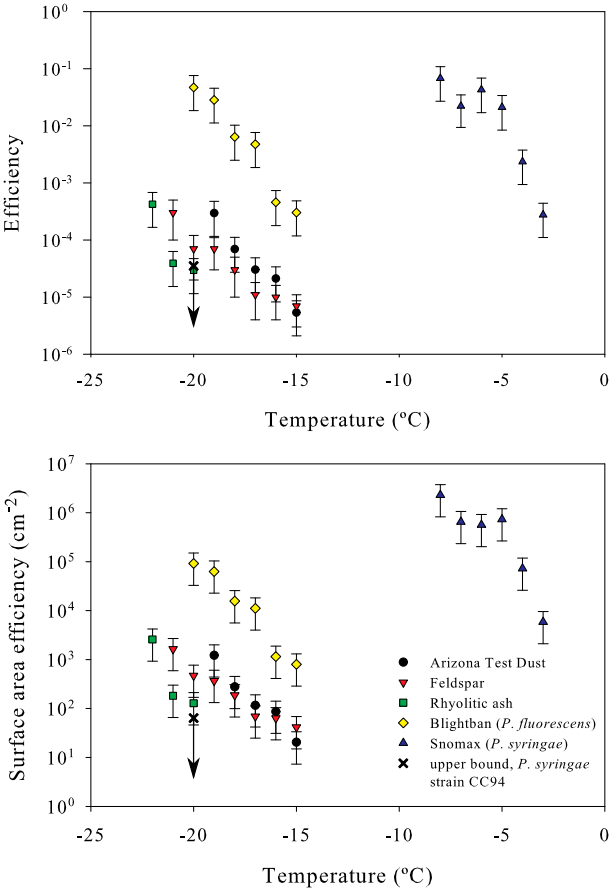

FIG. 1. (top) The freezing efficiency for three mineral dusts and three samples of bacteria. The mineral dusts are relatively inefficient ice nuclei in contact mode for $T > -20$°C. *P. fluorescens* is two to three orders of magnitude more effective by number at all temperatures tested. Efficiency for *P. fluorescens* and *P. syringae* is plotted as a function of the number of aerosol particles that collided with the droplet, not the number of cells. Larger particles are most likely clumps of individual cells. The contact-freezing limit is shown for the CC94 strain of *P. syringae*, based on the tests that we have run in which no freezing was observed. Snomax (*P. syringae*) is the most effective high-temperature ice nucleus, plateauing at 0.05 by −8°C. (bottom) As in the top panel, but for surface area freezing efficiency.

a. Number efficiency

The efficiency by number shown in the top panel of Fig. 1 can be interpreted as the probability that a single

particle–droplet collision will result in a freezing event. If it is the collision itself that catalyzes the freezing event, the probability of freezing should scale with the number of aerosol particles that have collided with the supercooled droplet.

All three mineral samples—ATD, feldspar, and rhyolitic ash—had similar nucleating efficiencies across the range of temperatures tested in this study. At −15°C, the mineral dusts have an efficiency of about 10^{-5}, and, as expected, E increases with decreasing temperature. If extrapolated to a temperature of −32°C, the dust would have an efficiency of 0.01. In comparison, Hoffmann et al. (2013a) report freezing efficiencies ranging from 0.04 to 0.4 for illite particles with mobility diameters ranging from 322 to 750 nm, respectively.

The bacterium *P. fluorescens* A506 had higher efficiencies than the dusts at all of the temperatures evaluated, with $E \simeq 0.05$ at −20°C. This result is especially striking when considering that this particular strain of *P. fluorescens* is ice negative; it does not possess the gene necessary for synthesis of the ice-nucleating protein in the cell membrane. While there are strains of *P. fluorescens* that are ice positive and exhibit high-temperature ice nucleation, they were not included in this study. Our results with strain A506 are remarkable because they suggest that some ice-negative bacteria may be more effective than dust in their ice-nucleating efficiency for $-15° > T > -20$°C.

Two strains of *P. syringae* were also tested and found to have widely varying efficiencies. Both are ice positive, as determined by nucleation tests in the immersion mode and in comparison to the results reported by Maki et al. (1974). Snomax starts to exhibit ice-nucleating activity in contact mode at −2.5°C, rising to $E = 0.1$ by −8°C. Some previous work with biological ice nuclei such as Snomax showed that they contain an average of one nucleation site per bacterial cell (Lagriffoul et al. 2010), but more recent experiments have indicated a maximum activated fraction in the immersion mode from 0.2 to 0.4 (Hartmann et al. 2013). In contrast, strain CC94 showed no freezing events in contact mode, at temperatures down to −20°C. The upper limits for E and SE for strain CC94 are shown with a cross in Fig. 1.

Even though *P. syringae* strain CC94 is ice positive, not every cell within a population expresses the ice nucleation gene, leading to the formation of the ice-nucleating protein at a given time. Previous work has shown that the immersion-freezing threshold decreases with a decreasing number of cells in a test droplet (Maki et al. 1974). Following Maki et al.'s procedure of determining the freezing temperatures of serial dilutions of samples, we have determined that the fraction of cells in our sample of CC94 that express the ice nucleation active gene is 2×10^{-6} (data not shown). This small fraction makes a statistically valid determination of E for CC94 time prohibitive. The fact that we see no contact nucleation from this strain at −20°C also indicates that the cells of *P. syringae* CC94 that do not express the ice nucleation active gene are not as effective in the contact mode as are the *P. fluorescens* A506 (BlightBan) cells, which are naturally deficient in the gene. However, we cannot rule out the possibility that the physical or chemical characteristics of the various bacterial samples influenced the results. For example, the freeze-dried samples of *P. syringae* CC94 used in this study were ground with a mortar and pestle, and this likely disrupted the association of the ice nucleation protein with the cell membrane that appears to be critical in maintaining the ice-nucleating capabilities of *P. syringae* strains at warmer temperatures in many cells. On the other hand, according to information provided by the manufacturer, the *P. fluorescens* A506 (BlightBan) samples contain 29% inactive ingredients, which is presumably primarily culture media components that would have depressed the freezing temperature of these samples. In contrast, the *P. syringae* CC94 cells used in this study were suspended in distilled and deionized water prior to freeze drying. Nevertheless, these results highlight the inherent variability in the ice-nucleating efficacy of biological material.

b. Surface area efficiency

As noted above, the efficiency can be interpreted as the probability that a single collision between an aerosol particle and a supercooled droplet of water will result in a freezing event. This interpretation is valid if it is solely the impact with the surface that catalyzes the freezing event. If however, there is some property of the surface of the aerosol particle that catalyzes the phase transition upon contact with the surface of the supercooled droplet of water, then the number of observed freezing events should scale with the surface area of the particles that have been deposited to the droplet.

To that end, consider Fig. 2, which shows representative number distributions (top panel) and surface area distributions (bottom panel) for Arizona Test Dust and BlightBan, as sampled by the OPS after the contact IN chamber. As noted in section 2c, the distributions that pass through the CINC and are observed by the OPS are a convolution of their representation in the parent sample, the probability that they are lofted into the airstream by the membrane, and their penetration efficiency through the sample system. The latter two dominate, so it is not surprising that the distributions for all of the dusts that we sampled are similar. That, however, facilitates comparison of their contact efficiencies.

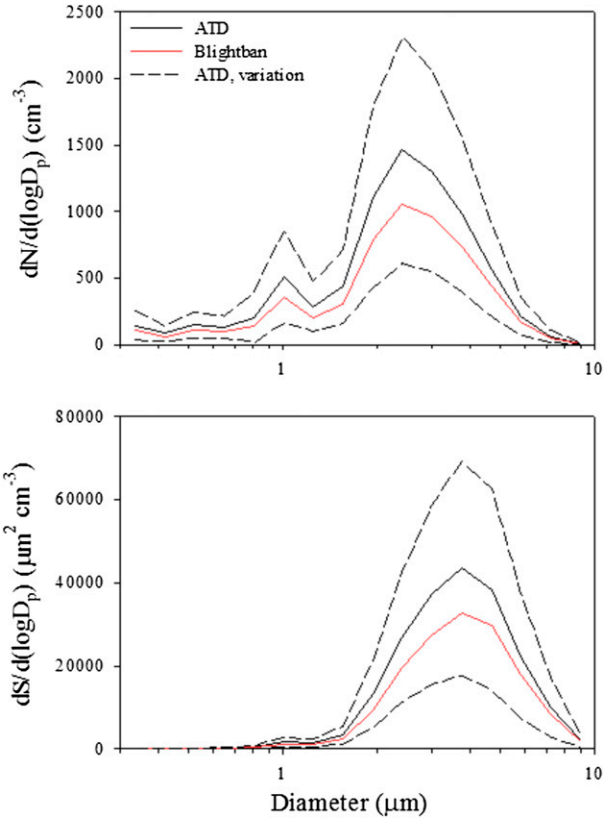

FIG. 2. (top) Representative number and (bottom) surface area distributions for ATD and BlightBan for a single experiment. The other dusts had similar number distributions. The mean is shown as a solid line; variation about the mean for the ATD (one standard deviation) during the experiment is shown with dashed lines. Variation about the mean was similar for other dusts.

The mode of the number distribution is at a diameter of about 2.5 μm, with a secondary peak at 1 μm. The secondary peak is much less important for the surface area, and the peak of the distribution shifts to about 4 μm. As expected, larger particles assume a greater importance, though the number of the largest particles (8–10 μm in diameter) is still so small that they contribute little to the overall surface area.

The surface area reported in the bottom panel of Fig. 2 is the geometric surface area, derived from the particle diameters reported by the OPS. For spherical particles of a specified index of refraction, the scattering signal is well known (Bohren and Huffman 1998). Mineral dust particles, are, however, not spherical; they have irregular shapes. We do not have the ability to correct for asphericity and so report the surface areas of the spheres. Mineral dust particles may also absorb incident radiation, which skews the size reported by the OPS, which is calibrated with polystyrene latex spheres. We used the OPS's internal correction for the index of refraction together with optical constants for ATD reported by Glen and Brooks (2013) to estimate the uncertainty associated with using the surface area derived from the standard calibration. Using the optical constants that include absorption shifts the diameters to a slightly higher value (~10%), which results in the total surface area increasing by approximately 15%, well within the range of the uncertainty shown in the bottom panel of Fig. 1. (We do not have optical constants for all the dusts, and so we cannot correct them all for absorption effects.)

The data for SE in the bottom panel of Fig. 1 show features similar to those exhibited by E. At −15°C, for every square centimeter of mineral dust surface area, deposited to the surface of a test droplet, there are 20 freezing events, rising to more than 1000 cm^{-2} at −20°C. *P. fluorescens* A506 (BlightBan) is, again, clearly separated from the inorganic particles; for a given quantity of material of the same size, for a given temperature, it is more than an order of magnitude more likely to catalyze freezing than are the mineral dusts. The BlightBan can nucleate ice at −15°C with SE = 10^3 cm^{-2}, whereas mineral dust requires almost another 5°C of cooling to achieve the same efficiency.

4. Atmospheric relevance

As Fig. 1 shows, few of the mineral dust particles are effective as contact-freezing nuclei in the temperature range from −15° to −20°C. Contact freezing is unlikely for a single particle–droplet collision, but our tests show that immersion freezing is even less likely (see section 2) in that temperature range. [See also the results in Hoffmann et al. (2013b).] As an upper limit on the production of ice by contact freezing by the dusts, consider a dust concentration of 1 cm^{-3} (DeMott et al. 2003) in a cloud with a droplet concentration of 100 cm^{-3} (Lamb and Verlinde 2011, chapter 1). Further assume that every dust particle is eventually collected by a cloud droplet during the lifetime of the cloud. At −20°C, E is just over 5×10^{-4} for the mineral dusts. For simplicity, we will round this to $E = 10^{-3}$, which leads to one nucleation event by the contact mechanism for every liter of cloudy air. Field observations of the number concentration of ice crystals produced by nucleation, not secondary mechanisms, in clouds ranges from about 0.01 to 10 L^{-1} of cloudy air at −20°C (Lamb and Verlinde 2011, p. 459).

Bacteria have the potential to be more significant IN. The efficiencies for *P. fluorescens* A506 reported here are, on average, more than an order of magnitude higher than those of the mineral dusts. The number concentrations of bacteria in the atmosphere are much more uncertain. However, if we estimate that the number concentration of bacteria is 100 times lower than

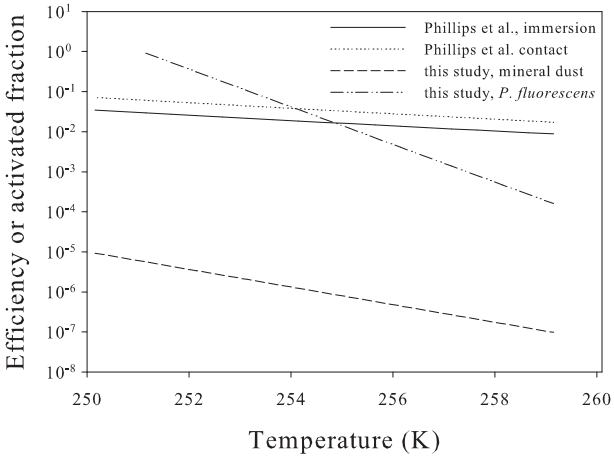

FIG. 3. Comparison of the data presented in this study with the parameterization from Phillips et al. (2008), based on measurements of submicron aerosol particles in the atmosphere. The activated fraction (our efficiency) of the mineral dust is three to five orders of magnitude lower than either the parameterized immersion or contact mode from Phillips et al. (2008) across the temperature range for which our measurements are valid.

mineral dust (Phillips et al. 2008, appendix C), that would still yield approximately one nucleation event per 2 L of cloudy air at −20°C. Snomax would produce 10 ice crystals per 1 L at −10°C. The high-temperature freezing events ($T > -10$°C) are particularly interesting because they occur in the temperature range of the most well-documented ice multiplication process, Hallett–Mossop. While these simple back-of-the-envelope examples do not prove that contact nucleation will lead to ice formation at temperatures of mixed-phase clouds, it does, at least, suggest that contact nucleation may play a role. More definitive conclusions will probably only be possible by incorporating realistic contact nucleation parameterizations into cloud-modeling studies.

Finally, Fig. 3 is a comparison between our mineral dust and *P. fluorescens* data and a parameterization of naturally occurring ice nuclei. Our data are shown as two best-fit lines, while the parameterization is from Phillips et al. (2008), which is based on measurements of ice nuclei and the surface area of natural aerosols. The parameters for the best-fit lines to our data are shown in Table 1. We used representative number distributions to derive the activated fraction from the parameterization for comparison to our freezing efficiencies. Note that Phillips et al. (2008) is based on measurements made with a continuous-flow diffusion chamber, which has an upper limit of 1 μm. The active fractions reported here are biased high because we used values of the surface area and total number of aerosol particles derived from our measurements, which are dominated by particles with diameters greater than 1 μm.

TABLE 1. Parameters for the best-fit lines to the mineral dust and *P. fluorescens* contact-nucleation data. The lines are of the form $\log(E) = b + aT$. We have grouped the mineral dust together; the individual datasets are similar enough as to be represented by a single line.

Substance	Intercept	Slope
Mineral dust	50 ± 10	−0.22 ± 0.04
P. fluorescens	120 ± 10	−0.47 ± 0.05

Comparison of our data with the parameterization from Phillips et al. (2008) suggests that dust aerosol in the atmosphere is three to five orders of magnitude more likely to catalyze a freezing event than are the laboratory-generated dust aerosols. Approximately 1%–3% of naturally occurring aerosol particles initiate freezing while the efficiency of contact nucleation that we measured ranges from 10^{-5} to 10^{-7}. Though our efficiencies are much smaller than those derived from the formulation of Phillips et al., the temperature sensitivity is much greater, increasing by two orders of magnitude over 9°C, whereas the parameterization increases by only a factor of 4. Though our *P. fluorescens* efficiencies are roughly 10 times lower than the frozen fractions from Phillips et al. (2008) for mineral dust at −14°C, they exceed the values at the lowest temperatures tested.

The contrast between the efficiencies that we measure for the dust and those predicted by Phillips et al.'s parameterization highlights the need for further investigation of this topic. Figure 3 clearly shows a large discrepancy between measured and predicted rates of contact nucleation, though the freezing efficacy of an ice-negative bacterium that we document in this study may provide an avenue for resolution. Recent work (Conen et al. 2011; O'Sullivan et al. 2013) indicates that material that would be classified as mineral dust in the scheme of Phillips et al. (2008) may have ice-nucleating activity from the biological residues associated with it.

5. Conclusions

We have quantified the fraction of aerosol particles that catalyze freezing in contact mode for three mineral dusts and three strains of bacteria for $T \geq -20$°C. For Arizona Test Dust, feldspar, or rhyolitic ash, the freezing efficiency E is less than 10^{-3} for −20°C, decreasing to less than 10^{-5} at −15°C. In contrast to the mineral dusts, an ice-negative strain of *Pseudomonas fluorescens* is an order of magnitude more effective at every temperature tested, rising to $E \simeq 0.1$ at −20°C. Another commercially available bacterium, Snomax (*Pseudomonas syringae*), reaches that value 12°C higher than does the *Pseudomonas fluorescens*,

similar to what is seen with ice-negative and ice-positive bacteria in immersion mode. The cells of *Pseudomonas syringae* CC94 that did not express the ice-nucleating gene showed no contact-freezing activity, whereas the ice-negative strain of *Pseudomonas fluorescens* did, which highlights the inherent variability within biological material.

Our contact-nucleation efficiencies for mineral dust are three to five orders of magnitude lower than those derived from a parameterization of ice nucleation activity in contact mode as determined from field measurements (Phillips et al. 2008). (The field measurements and parameterization also show significantly higher efficiencies for immersion mode in the temperature range investigated.) Our measurements of the contact freezing efficiency of both ice-positive and ice-negative bacteria may help to explain this discrepancy, as biological material present on atmospheric dusts could increase their efficacy considerably.

Acknowledgments. This work was funded through the National Science Foundation: AGS-1028998, AGS-1039742, and AGS-1119164. Ashima Chhabra, who was funded through the Michigan University College Partnership program in the summer of 2012, helped with some of the ice nucleation tests with *P. syringae*. Adam Cary cultured the *P. syringae* CC94 and was supported through funds internal to Michigan Tech, including SURF in the summer of 2013. Thanks also to Adam Durant for giving us the sample of rhyolitic ash; similarly, thanks to Thomas Whale and Benjamin Murray for the sample of feldspar. Thanks to David Sands who provided the sample of *P. syringae* CC94. Nufarm Americas graciously provided a sample of BlightBan A506. Finally, we appreciate the thorough, constructive reviews that helped us to improve the paper.

REFERENCES

Atkinson, J. D., and Coauthors, 2013: The importance of feldspar for ice nucleation by mineral dust in mixed-phase clouds. *Nature,* **498,** 355–358, doi:10.1038/nature12278.

Bohren, C., and D. Huffman, 1998: *Absorption and Scattering of Light by Small Particles.* John Wiley and Sons, 544 pp.

Bunker, K. W., S. China, C. Mazzoleni, A. Kostinski, and W. Cantrell, 2012: Measurements of ice nucleation by mineral dusts in the contact mode. *Atmos. Chem. Phys. Discuss.,* **12,** 20 291–20 309, doi:10.5194/acpd-12-20291-2012.

Conen, F., C. E. Morris, J. Leifeld, M. V. Yakutin, and C. Alewell, 2011: Biological residues define the ice nucleation properties of soil dust. *Atmos. Chem. Phys.,* **11,** 9643–9648, doi:10.5194/acp-11-9643-2011.

Cooper, W., 1974: A possible mechanism for contact nucleation. *J. Atmos. Sci.,* **31,** 1832–1837, doi:10.1175/1520-0469(1974)031<1832:APMFCN>2.0.CO;2.

DeMott, P. J., K. Sassen, M. R. Poellot, D. Baumgardner, D. C. Rogers, S. D. Brooks, A. J. Prenni, and S. M. Kreidenweis, 2003: African dust aerosols as atmospheric ice nuclei. *Geophys. Res. Lett.*, **30,** 1732, doi:10.1029/2003GL017410.

Després, V. R., and Coauthors, 2012: Primary biological aerosol particles in the atmosphere: A review. *Tellus,* **64B,** 15598, doi:10.3402/tellusb.v64i0.15598.

Fornea, A., S. Brooks, J. Dooley, and A. Saha, 2009: Heterogeneous freezing of ice on atmospheric aerosols containing ash, soot, and soil. *J. Geophys. Res.,* **114,** D13201, doi:10.1029/2009JD011958.

Fukuta, N., 1975: A study of the mechanism of contact nucleation. *J. Atmos. Sci.,* **32,** 1597–1603, doi:10.1175/1520-0469(1975)032<1597:ASOTMO>2.0.CO;2.

Glen, A., and S. D. Brooks, 2013: A new method for measuring optical scattering properties of atmospherically relevant dusts using the Cloud and Aerosol Spectrometer with Polarization (CASPOL). *Atmos. Chem. Phys.,* **13,** 1345–1356, doi:10.5194/acp-13-1345-2013.

Gokhale, N., and J. Goold Jr., 1968: Droplet freezing by surface nucleation. *J. Appl. Meteor.,* **7,** 870–874, doi:10.1175/1520-0450(1968)007<0870:DFBSN>2.0.CO;2.

——, and J. Spengler, 1972: Freezing of freely suspended, supercooled water drops by contact nucleation. *J. Appl. Meteor.,* **11,** 157–160, doi:10.1175/1520-0450(1972)011<0157:FOFSSW>2.0.CO;2.

Hartmann, S., S. Augustin, T. Clauss, H. Wex, T. Šantl Temkiv, J. Voigtländer, D. Niedermeier, and F. Stratmann, 2013: Immersion freezing of ice nucleation active protein complexes. *Atmos. Chem. Phys.,* **13,** 5751–5766, doi:10.5194/acp-13-5751-2013.

Hoffmann, N., D. Duft, A. Kiselev, and T. Leisner, 2013a: Contact freezing efficiency of mineral dust aerosols studied in an electrodynamic balance: quantitative size and temperature dependence for illite particles. *Faraday Discuss.,* **165,** 383–390, doi:10.1039/C3FD00033H.

——, A. Kiselev, D. Rzesanke, D. Duft, and T. Leisner, 2013b: Experimental quantification of contact freezing in an electrodynamic balance. *Atmos. Meas. Tech.,* **6,** 2373–2382, doi:10.5194/amt-6-2373-2013.

Hoose, C., and O. Möhler, 2012: Heterogeneous ice nucleation on atmospheric aerosols: A review of results from laboratory experiments. *Atmos. Chem. Phys. Discuss.,* **12,** 12 531–12 621, doi:10.5194/acpd-12-12531-2012.

Joly, M., E. Attard, M. Sancelme, L. Deguillaume, C. Guilbaud, C. E. Morris, P. Amato, and A.-M. Delort, 2013: Ice nucleation activity of bacteria isolated from cloud water. *Atmos. Environ.,* **70,** 392–400, doi:10.1016/j.atmosenv.2013.01.027.

King, E. O., M. Ward, and D. Raney, 1954: Two simple media for the demonstration of pyocyanin aind fluorescin. *J. Lab. Clin. Med.,* **44,** 301–307.

Korolev, A. V., G. A. Isaac, S. G. Cober, J. W. Strapp, and J. Hallett, 2003: Microphysical characterization of mixed-phase clouds. *Quart. J. Roy. Meteor. Soc.,* **129,** 39–65, doi:10.1256/qj.01.204.

Ladino, L., O. Stetzer, F. Lüönd, A. Welti, and U. Lohmann, 2011: Contact freezing experiments of kaolinite particles with cloud droplets. *J. Geophys. Res.,* **116,** D22202, doi:10.1029/2011JD015727.

Ladino Moreno, L. A., O. Stetzer, and U. Lohmann, 2013: Contact freezing: A review of experimental studies. *Atmos. Chem. Phys.,* **13,** 9745–9769, doi:10.5194/acp-13-9745-2013.

Lagriffoul, A., and Coauthors, 2010: Bacterial-based additives for the production of artificial snow: What are the risks to human health? *Sci. Total Environ.,* **408,** 1659–1666, doi:10.1016/j.scitotenv.2010.01.009.

Lamb, D., and J. Verlinde, 2011: *Physics and Chemistry of Clouds.* Cambridge University Press, 584 pp.

Levin, Z., and S. A. Yankofsky, 1983: Contact versus immersion freezing of freely suspended droplets by bacterial ice nuclei. *J. Climate Appl. Meteor.,* **22,** 1964–1966, doi:10.1175/1520-0450(1983)022<1964:CVIFOF>2.0.CO;2.

Lohmann, U., 2002: A glaciation indirect aerosol effect caused by soot aerosols. *Geophys. Res. Lett.*, **29,** doi:10.1029/2001GL014357.

Maki, L. R., E. L. Galyan, M.-M. Chang-Chien, and D. R. Caldwell, 1974: Ice nucleation induced by pseudomonas syringae. *Appl. Microbiol.,* **28** (3), 456–459.

Morris, C., 2012: Interactive comment on ''Heterogeneous ice nucleation on atmospheric aerosols: A review of results from laboratory experiments'' by C. Hoose and O. Möhler. *Atmos. Chem. Phys. Discuss.,* **12,** C3025–C3027.

Niehaus, J., K. Bunker, S. China, A. Kostinski, C. Mazzoleni, and W. Cantrell, 2013: A technique to measure ice nuclei in the contact mode. *J. Atmos. Oceanic Technol.,* **31,** 913–922, doi:10.1175/JTECH-D-13-00156.1.

O'Sullivan, D., and Coauthors, 2013: Ice nucleation by soil dusts: relative importance of mineral dust and biogenic components. *Atmos. Chem. Phys. Discuss.,* **13,** 20 275–20 317, doi:10.5194/acpd-13-20275-2013.

Phillips, V., P. DeMott, and C. Andronache, 2008: An empirical parameterization of heterogeneous ice nucleation for multiple chemical species of aerosol. *J. Atmos. Sci.,* **65,** 2757–2783, doi:10.1175/2007JAS2546.1.

Pitter, R., and H. Pruppacher, 1973: A wind tunnel investigation of freezing of small water drops falling at terminal velocity in air. *Quart. J. Roy. Meteor. Soc.,* **99,** 540–550, doi:10.1002/qj.49709942111.

Svensson, E., C. Delval, P. von Hessberg, M. Johnson, and J. Pettersson, 2009: Freezing of water droplets colliding with kaolinite particles. *Atmos. Chem. Phys.,* **9,** 4295–4300, doi:10.5194/acp-9-4295-2009.

Vali, G., M. Christensen, R. W. Fresh, E. L. Galyan, L. R. Maki, and R. C. Schnell, 1976: Biogenic ice nuclei. Part II: Bacterial sources. *J. Atmos. Sci.,* **33,** 1565–1570, doi:10.1175/1520-0469(1976)033<1565:BINPIB>2.0.CO;2.

Yun, Y., and J. E. Penner, 2012: Global model comparison of heterogeneous ice nucleation parameterizations in mixed phase clouds. *J. Geophys. Res.*, **117,** D07203, doi:10.1029/2011JD016506.